1 # Technical Note: Preventing CO_2 overestimation from mercuric or

2 # copper (II) chloride preservation of dissolved greenhouse gases in

3 # freshwater samples

4

5 François Clayer[1*], Jan Erik Thrane[1], Kuria Ndungu[1], Andrew King[1], Peter Dörsch[2], Thomas Rohrlack[2]

6

7 [1]Norwegian Institute for Water Research (NIVA), Økernveien 94, 0579 Oslo, Norway

8

9 [2]Faculty of Environmental Sciences and Natural Resource Management, Norwegian University of

10 Life Sciences, PO Box 5003, 1432 Ås, Norway

11

12 [*]Corresponding author(s): François Clayer (francois.clayer@niva.no)

13

14 **Abstract**

15 The determination of dissolved gases (O_2, CO_2, CH_4, N_2O, N_2) in surface waters allows to estimate

16 biological processes and greenhouse gas fluxes in aquatic ecosystems. Mercuric chloride ($HgCl_2$) has

17 been widely used to preserve water samples prior to gas analysis. However, alternates are needed

18 because of the environmental impacts and regulation of mercury. $HgCl_2$ is a weak acid and interferes

19 with dissolved organic carbon (DOC). Hence, we tested the effect of $HgCl_2$ and two substitutes

20 (copper (II) chloride – $CuCl_2$ and silver nitrate – $AgNO_3$), as well as storage time (24h to 3 months)

21 on the determination of dissolved gases in low ionic strength and high DOC lake water. Furthermore,

22 we investigated and predicted the effect of $HgCl_2$ on CO_2 concentrations in periodic samples from

23 another lake experiencing pH variations (5.4–7.3) related to *in situ* photosynthesis. Samples fixed

24 with inhibitors generally showed negligible O_2 consumption. However, effective preservation of

25 dissolved CO_2, CH_4 and N_2O for up to three months prior to dissolved gas analysis, was only achieved

26 with $AgNO_3$. In contrast, $HgCl_2$ and $CuCl_2$ caused an initial increase in CO_2 and N_2O followed by a

27 decrease. The CO_2 overestimation, caused by $HgCl_2$-acidification and shift in the carbonate

28 equilibrium, can be calculated from predictions of chemical speciation. Errors due to CO_2

29 overestimation in $HgCl_2$-preserved water, sampled from low ionic strength and high DOC freshwater,

30 could lead to an overestimation of the CO_2 diffusion efflux by a factor of >20 over a month, or a

31 factor of 2 over the ice-free season.

32

33 **Key-words**: lake, greenhouse gases, water sample preservation, mercuric chloride, metal toxicity,

34 carbon dioxide

CO_2 overestimation from $HgCl_2$ fixation – Clayer et al.

35   **Running tile**: CO_2 overestimation from $HgCl_2$ fixation

36 **1 Introduction**

37

38 The determination of dissolved gases by gas chromatography from samples collected in the field

39 allows the estimation of biological processes in aquatic ecosystems such as photosynthesis and oxic

40 respiration (O_2, CO_2), denitrification (N_2, N_2O) and methanogenesis (CH_4). This technique is also

41 useful to test the calibration of *in-situ* sensors in long term deployment. The partial pressure of these

42 dissolved gases will continue to evolve in the water sample from the time of collection to the time of

43 analysis unless biological activity is prevented. This is an issue when field sites are far from

44 laboratory facilities, and it may be more efficient to process the samples in large batches at the end of

45 the field season.

46 Mercuric (II) chloride ($HgCl_2$) has been widely used as an inhibitor of the above-mentioned biological

47 processes to preserve water samples for the determination of dissolved CO_2 in seawaters (e.g.

48 Dickson, Sabine & Christian, 2007) and several dissolved gases in natural and artificial freshwater

49 bodies (e.g. O_2, CO_2, CH_4, N_2 and/or N_2O; (Guérin et al., 2006; Hessen et al., 2017; Hilgert et al.,

50 2019; Okuku et al., 2019; Schubert et al., 2012; Xiao et al., 2014; Yan et al., 2018; Yang et al., 2015)

51 because it is extremely toxic at very low concentrations compared to other reagents (e.g. Horvatić &

52 Peršić, 2007; Hassen *et al.*, 1998). Worldwide efforts have sought to reduce the use of mercury

53 because it is considered toxic to the environment and exposure can severely affect human health

54 (Chen et al., 2018). Therefore, alternative preservation techniques to $HgCl_2$ have been tested for

55 dissolved inorganic carbon (DIC) and δ^{13}C-DIC such as acidification with phosphoric acid (Taipale &

56 Sonninen, 2009) or a combination of filtration and exposure to benzalkonium chloride or sodium

57 chloride (Takahashi *et al.*, 2019). At least two studies, one also including dissolved organic carbon

58 (DOC) and δ^{13}C-DOC, showed that simple filtration (and cooling), fixation (precipitation) or

59 acidification were better than the use of toxic inhibitors, including $HgCl_2$ (Wilson, Munizzi & Erhardt,

60 2020). However, these techniques were not tested for the simultaneous determination of several

61 dissolved gases, including CH_4 which is subject to rapid degassing during handling or storage if

62 samples are not preserved because of its low solubility in water (Duan & Mao, 2006).

63 The addition of $HgCl_2$ to water is known to produce hydrochloric acid through hydrolysis (Ciavatta &

64 Grimaldi, 1968) and to form complexes with many environmental ligands, both inorganic (Powell *et*

65 *al.*, 2004) and organic (Tipping, 2007; Foti *et al.*, 2009; Liang *et al.*, 2019; Chen *et al.*, 2017). The

66 complexation of Hg^+ with the carboxyl or thiol groups of dissolved organic carbon in oxic

67 environments could further increase the concentration of H^+ (Khwaja et al., 2006; Skyllberg, 2008).

68 This acidification could be an issue in poorly buffered water (low ionic strength) with high

69 concentration of DOC where a shift in the pH and carbonate equilibrium could be induced, thus

70 resulting in an overestimation of dissolved CO_2 concentration. Such effects would not be expected in

71 marine water due to the high ionic strength of the water (Chou *et al.*, 2016) or freshwater with low pH

CO$_2$ overestimation from HgCl$_2$ fixation – Clayer et al.

72   (<5.5) under which conditions nearly all dissolved inorganic carbon is CO$_2$ (Stumm & Morgan, 1981).

73   Thus, there are clear limits of the application of HgCl$_2$ for freshwater preservation, in addition to

74   exposing field workers to the risks of its high toxicity.

75   The use of HgCl$_2$ to preserve water samples prior to dissolved gas analyses is part of the current

76   guidelines for greenhouse gas measurements in freshwater reservoirs (Machado Damazio et al., 2012;

77   UNESCO/IHA, 2008, 2010). Hence, there is a risk of overestimating CO$_2$ concentrations and

78   emissions, in absence of discrete measurement of emissions, from hydropower reservoirs with

79   consequence on the present and expected greenhouse gas footprint from hydroelectricity. To ensure

80   precise estimation of greenhouse gas emission from hydropower, the largest present and future

81   renewable source of electricity (IEA, 2020), the use of HgCl$_2$ should therefore be discontinued.

82   Here we tested the effect of storage of a natural water sample with circumneutral pH, low ionic

83   strength (poor buffering capacity) and high DOC concentration on the determination of five dissolved

84   gases (O$_2$, CO$_2$, CH$_4$, N$_2$ and N$_2$O) by headspace equilibration and gas chromatography in the

85   presence of mercuric chloride (HgCl$_2$), two alternative inhibitors, chosen for their wide and effective

86   application in water treatments and water purification (copper (II) chloride – CuCl$_2$ and silver nitrate –

87   AgNO$_3$; Xu & Imlay, 2012; Rai, Gaur & Kumar, 1981), and a control (samples chilled in the dark at

88   +4°C). We further investigated the effect of preservation with HgCl$_2$ on the determination of

89   dissolved CO$_2$ from water samples collected weekly during a full ice-free season from a lake

90   experiencing varying pH conditions related to photosynthesis. Finally, we show that the

91   overestimation of dissolved CO$_2$ concentrations caused by HgCl$_2$ fixation can be predicted based on

92   chemical equilibria.

93

94   **2. Methods**

95   2.1. Effects of storage time and inhibitors on the determination of dissolved gases

96   *Study area*

97   Water samples were collected from Lake Svartkulp (59.9761313 N, 10.7363544 E; Southeast

98   Norway) north of Oslo, Norway, on the 4th of September 2019. Lake water was carefully collected

99   into 5 L plastic bottles to avoid sampling large particles and immediately brought back to the lab.

100   Upon arrival at the laboratory, water from the 5 L bottles were slowly poured, to avoid gas loss, into a

101   25 L tank to provide a single bulk sample to start the incubation experiment. Filtration, e.g., with 0.45

102   or 0.2 μm filters, was avoided to minimize changes in dissolved gas concentrations (e.g., Magen et al.,

103   2014). The mixed water sample (25 L) was sub-sampled (0.5 L) for the determination of alkalinity

104   (127 μmol L^{-1}), pH (6.73), ammonium (3 μg N L^{-1}), nitrate (5 μg N L^{-1}), total N (230 μg N L^{-1}),

105   phosphate (1 μg P L^{-1}), total P (9 μg P L^{-1}), TOC (8.9 mg C L^{-1}) and colour (59 mg L^{-1} Pt), all

CO_2 overestimation from $HgCl_2$ fixation – Clayer et al.

106 analysed by standard methods at the accredited NIVA lab (see Table S1). Temperature of the lake

107 water was 18.5 °C. Note that particulate organic carbon is a negligible fraction of TOC in Norwegian

108 lake waters, representing less than 3% (de Wit et al., 2023).

109

110 *Laboratory experiment*

111 The experimental design involved four treatments ($HgCl_2$, $CuCl_2$, $AgNO_3$ and control, i.e., no added

112 preservative), three time points of dissolved gas analysis (t=0, i.e., within 24h, t= 3 weeks and t = 3

113 months) and six replicates, yielding in total 72 experimental units. The same day as the water samples

114 were collected, water from the mixed sample (25 L) was added gently to 72 borosilicate glass bottles

115 (120 mL) and the bottles were randomized.

116 Stock solutions of $HgCl_2$, $CuCl_2$ and $AgNO_3$ were prepared according to Table 1. For measurement of

117 CO_2 in seawater samples, the standard method involves poisoning the samples by adding a saturated

118 $HgCl_2$ solution in a volume equal to 0.05-0.02% of the total volume (Dickson 2007). We used this as

119 a starting point and added 0.02 % saturated $HgCl_2$ solution to 1/4th of the samples (240 μL of $HgCl_2$

120 10× diluted saturated solution), resulting in a sample concentration of 14 μg $HgCl_2$ mL^{-1} (51.6 μM;

121 Table 1). Based on estimated toxicity relative to Hg (Deheyn et al., 2004; Halmi et al., 2019), the

122 silver and copper salts were added in molar concentrations equal to two and three times the molar

123 concentration of $HgCl_2$, respectively (Table 1), although it varies between species of microorganisms

124 and environmental matrices (Hassen *et al.*, 1998; Rai, Gaur & Kumar, 1981). $CuCl_2$ and $AgNO_3$, the

125 most toxic form of Silver, were chosen because of their wide application in water treatments and

126 water purification (Larrañaga et al., 2016; Nowack et al., 2011; NPIRS, 2023; Ullmann et al., 1985).

127 Equal volume of MilliQ water was added to 1/4th of the samples as a control. The bottles were capped

128 with gas tight butyl rubber stoppers after ensuring that there were no air bubbles in the samples. The

129 samples for measurement of starting concentrations (t=0) were stored dark and cold (+4°C) overnight

130 and analyzed within 24h of preparation, while the rest were stored dark and cold (+4°C) until

131 measurement after 3 weeks (t= 3w) and 3 months (t= 3m) of storage. Concentrations of O_2, N_2, N_2O,

132 CO_2 and CH_4 were determined by gas chromatography (see below) using the headspace technique

133 following Yang *et al.* (2015). Unfortunately, pH was not measured at the end of the storage period.

134 **Table 1.** Stock and sample concentrations of $HgCl_2$, $CuCl_2$ and $AgNO_3$.

Salt	Stock solution	Sample concentration	Rationale
$HgCl_2$	70 g/L (saturated)	14.0 μg/mL (51.6 μM)	Dickson, Sabine & Christian, 2007
$CuCl_2$	131.9 g/L	26.4 μg/mL (154.7 μM)	3 × Hg
$AgNO_3$	87.6 g/L	17.5 μg/mL (103.1 μM)	2 × Hg

135

CO_2 overestimation from $HgCl_2$ fixation – Clayer et al.

136   2.2. Effects of $HgCl_2$ on dissolved CO_2 analyses over a range of pH values

137   *Lake Lundebyvannet time series*

138   Water samples were collected from Lake Lundebyvannet located southeast of Oslo (59.54911 N,

139   11.47843 E, Southeast Norway). The lake has a surface area of 0.4 km^2 and a maximum depth of

140   5.5 m. Samples were taken from 1, 1.5, 2 and 2.5 m depth once or twice a week between April 2020

141   and January 2021. Samples for GC analysis were filled into 120 mL glass bottles, which were sealed

142   immediately without air bubbles. Sample preservation prior to GC analysis (within 24h) was ensured

143   by adding a half-saturated (at 20°C) solution of $HgCl_2$ (150 µL) through the rubber seal of each bottle

144   using a syringe directly after sampling, resulting in a concentration of 161 µM similar to previous

145   studies (Clayer et al., 2021; Hessen et al., 2017; Yang et al., 2015). Samples for DIC analysis were

146   filled without bubbles in 100 ml Winkler glass bottles that were sealed airtight directly after sampling.

147   These samples were not fixed in any way and were analysed by a TOC analyzer and a pH-meter

148   within two hours. The lake water was characterised by high concentrations of humic substances (with

149   DOC concentrations ranging from 8 to 28 mg C L^{-1}), weak ionic strength with alkalinity ranging

150   between 30 and 150 µmol L^{-1}, and electric conductivity varying from 40 to 70 µS cm^{-1}. Temperature

151   and pH were measured *in-situ* using a HOBO pH data logger placed at 1, 1.5, 2 and 2.5 m (Elit,

152   Gjerdrum, Norway). For more details, see Rohrlack *et al.* (2020).

153

154   2.3. Analytical chemistry

155   *Gas chromatography*

156   Headspace was prepared by gently backfilling sample bottles with 20–30 mL helium (He; 99,9999%)

157   into the closed bottle while removing a corresponding volume of water. Care was taken to control the

158   headspace pressure within 5% of ambient and a slight He overpressure was released before

159   equilibration. The bottles were shaken horizontally at 150 rpm for 1 h to equilibrate gases between

160   sample and headspace. The temperature during shaking was recorded by a data logger. Immediately

161   after shaking, the bottles were placed in an autosampler (GC-Pal, CTC, Switzerland) coupled to a gas

162   chromatograph (GC) with He back-flushing (Model 7890A, Agilent, Santa Clara, CA, US).

163   Headspace gas was sampled (approx. 2 mL) by a hypodermic needle connected to a peristaltic pump

164   (Gilson Minipuls 3), which connected the autosampler with the 250 µL heated sampling loop of the

165   GC.

166   The GC was equipped with a 20-m wide-bore (0.53 mm) Poraplot Q column for separation of CH_4,

167   CO_2 and N_2O and a 60 m wide-bore Molsieve 5Å PLOT column for separation of O_2 and N_2, both

168   operated at 38°C and with He as carrier gas. N_2O and CH_4 were measured with an electron capture

169   detector run at 375°C with Ar/CH_4 (80/20) as makeup gas, and a flame ionization detector,

170 respectively. CO$_2$, O$_2$, and N$_2$ were measured with a thermal conductivity detector (TCD). Certified

171 standards of CO$_2$, N$_2$O, and CH$_4$ in He were used for calibration (AGA, Germany), whereas air was

172 used for calibrating O$_2$ and N$_2$. The analytical error for all gases was lower than 2%. For the Lake

173 Lundebyvannet time series, CO$_2$ was separated from other gases using the 20 m wide-bore (0.53 mm)

174 Poraplot Q column while the other gases were not measured.

175 The results from gas chromatography give the relative concentration of dissolved gases (in ppm) in

176 the headspace in equilibrium with the water. For the lab experiment (section 2.1), the concentration of

177 dissolved gases in the water at equilibrium with the headspace were calculated from the solubility of

178 gases in water using Carroll, Slupsky and Mather (1991) for CO$_2$, Weiss and Price (1980) for N$_2$O,

179 Yamamoto, Alcauskas and Crozier (1976) for CH$_4$, Millero, Huang and Laferiere (2002) for O$_2$,

180 Hamme and Emerson (2004) for N$_2$. For the Lake Lundebyvannet time series (section 2.2), the

181 concentration of CO$_2$ in the water samples were determined using temperature-dependent Henry's law

182 constants given by Wilhelm, Battino and Wilcock (1977). The quantities of gases in the headspace

183 and water were summed to find the concentrations and partial pressures of dissolved gases from the

184 water collected in the field. The calculations were similar to Yang *et al.* (2015).

185

186 *DIC analyses*

187 DIC analysis was performed for the Lake Lundebyvannet time series using a Shimadzu TOC-V CPN

188 (Oslo, Norway) instrument equipped with a non-dispersive infrared (NDIR) detector with O$_2$ as a

189 carrier gas at a flow rate of 100 mL min^{-1}. Two to three replicate measurements were run per sample.

190 The system was calibrated using a freshly prepared solution containing different concentrations of

191 NaHCO$_3$ and Na$_2$CO$_3$. CO$_2$ concentrations in water samples ($[CO_2]$) were calculated on the bases of

192 temperature, pH and DIC concentrations as follows (Rohrlack *et al.*, 2020):

193
$$[CO_2] = \frac{[H^+]^2 C_T}{Z} \qquad \text{(Eq. 1)}$$

194 where $[H^+]$ is the proton concentration (10^{-pH}), C_T is the dissolved inorganic carbon concentration

195 and Z is given by:

196
$$Z = [H^+]^2 + K_1[H^+] + K_1K_2 \qquad \text{(Eq. 2)}$$

197 where K_1 and K_2 are the first and second carbonic acid dissociation constant adjusted for temperature

198 (pK$_1$ = 6.41 and pK$_2$ = 10.33 at 25°C; Stumm & Morgan, 1996).

199

200 2.4. Data analysis

201   *pCO$_2$ and saturation deficit*

202   Lake Lundebyvannet CO$_2$ concentrations provided by GC and DIC analyses were converted to pCO$_2$

203   (in µatm) as follows:

204
$$pCO_2 = \frac{[CO_2]}{0.987 \times K_H \, P_{atm}}$$
(Eq. 3)

205   where K_H is Henry constant for CO$_2$ adjusted for in-situ water temperature (Stumm & Morgan, 1996)

206   and P_{atm} is the atmospheric pressure in bar given by:

207
$$P_{atm} = (1013 - 0.1 \times altitude) \times 0.001$$
(Eq. 4)

208   where $altitude$ is the altitude of Lake Lundebyvannet (158 m). Finally, the CO$_2$ saturation deficit

209   (Sat_{CO_2} in µatm) was given by

210
$$Sat_{CO_2} = pCO_2 - [CO_2]_{air}$$
(Eq. 5)

211   where $[CO_2]_{air}$ is the pCO$_2$ in the air (416 µatm for 2020 in Southern Norway retrieved from EBAS

212   database; NILU, 2022; Tørseth et al., 2012). Sat_{CO_2} gives the direction of CO$_2$ flux at the air water

213   interface, and its product with gas transfer velocity determine the CO$_2$ flux at the water-atmosphere

214   interface, i.e., whether lake ecosystems are sink ($Sat_{CO_2} < 0$) or source ($Sat_{CO_2} > 0$) of atmospheric

215   CO$_2$.

216

217   *Statistical analyses*

218   The effect of storage time and treatment on five dissolved gases (O$_2$, N$_2$, CO$_2$, CH$_4$, N$_2$O) from the

219   Lake Svartkulp samples was tested with a two-way ANOVA at an alpha level adapted using the

220   Bonferroni correction for multiple testing, i.e., $\alpha = 0.05/5 = 0.01$. To evaluate the impact of Hg fixation

221   on Lake Lundebyvannet samples, $[CO_2]$ values determined by headspace equilibration and GC

222   analysis of HgCl$_2$-fixed samples were compared with those calculated from DIC measurements of

223   unfixed samples with a paired t-test.

224   A regression analysis was performed to describe the overestimation of CO$_2$ concentrations caused by

225   HgCl$_2$ fixation in Lake Lundebyvannet samples as a function of pH. The total CO$_2$ concentration in

226   the HgCl$_2$-fixed samples ($[CO_2]_{HgCl_2}$) can be expressed as:

227
$$[CO_2]_{HgCl_2} = [CO_2]_i + [CO_2]_{ex}$$
(Eq. 6)

228   where $[CO_2]_i$ is the initial CO$_2$ concentration prior to HgCl$_2$ fixation, i.e., CO$_2$ concentration in the

229   unfixed samples, and $[CO_2]_{ex}$ is the excess CO$_2$ concentration caused by a decrease in pH following

230   HgCl$_2$ fixation. The relative CO$_2$ overestimation (E) is given by:

CO$_2$ overestimation from HgCl$_2$ fixation – Clayer et al.

231
$$E = \frac{[CO_2]_{HgCl_2} - [CO_2]_i}{[CO_2]_i} = \frac{[CO_2]_{ex}}{[CO_2]_i} \qquad \text{(Eq. 7)}$$

232   The impact of pH (or $[H^+]$) on E was mathematically described by running a regression analysis

233   using MATLAB®. The *fminsearch* MATLAB function from the Optimization toolbox was used to

234   find the minimum sum of squared residuals (SSR) for functions of the form of: $E = A/[H^+]$ or $E =$

235    $A \times 10^{-B \times pH}$. For each optimal solution, the root-mean-square error (RMSE) and coefficient of

236   determination (R^2) were calculated against observed values of E, i.e., values of E determined

237   empirically from observed $[CO_2]_i$ and $[CO_2]_{ex}$.

238

239   *Chemical speciation, saturation-index calculations, and prediction of CO$_2$ overestimation*

240   The speciation of solutes and saturation index values (SI) of selected minerals were calculated with

241   the program PHREEQC developed by the USGS (Parkhurst & Appelo, 2013), neglecting the effect of

242   dissolved organic matter. This was used to assess the impact of the addition of preservative on shifting

243   the carbonate equilibrium as well as dissolved inorganic carbon losses due to carbonate mineral

244   precipitation. For each PHREEQC simulation, two files, respectively the database and input files,

245   were used to define the thermodynamic model and the type of calculations to perform. The database

246   of MINTEQA2 (e.g., *minteq.dat*, Allison et al., 1991) was used to describe the chemical system

247   because it includes, inter alia, reactions and constants for Ag, Cu and Hg complexation with Cl, NO$_3$

248   and carbonates. In total, three simulations were run representing the addition of each preservative

249   solution to sample water from Lake Svartkulp. The input files described the composition of two

250   aqueous solutions: (i) the preservative solution assumed to contain only the preservative and (ii)

251   sample water from Lake Svartkulp with observed major element concentrations (pH, Al, Ca, Cl, Cu,

252   Fe, Mg, Mn, N as nitrate, K, Na, S as sulfate, Zn; Table S1) and Hg and Ag concentration assumed to

253   be 10^{-5} mg/L. The output file provided the activities of the various solutes in the preserved samples,

254   i.e., simulating the mixing of 120 mL of lake water with 240 μL of the AgNO$_3$, CuCl$_2$ and HgCl$_2$

255   preservative solutions, as described in section 2.1. This procedure allows to estimate the pH of the

256   preserved samples as well as SI for various mineral phases. The SI is calculated by PHREEQC

257   comparing the chemical activities of the dissolved ions of a mineral (ion activity product, IAP) with

258   their solubility product (Ks). When SI > 1, precipitation is thermodynamic favourable. However,

259   PHREEQC does not give information about precipitation kinetics.

260   PHREEQC was also used to estimate the decrease in pH caused by adding 150 μL of a half-saturated

261   HgCl$_2$ solution to Lake Lundebyvannet samples prior to GC analyses, as described in section 2.2. In

262   absence of data on the chemical composition of Lake Lundebyvannet, we assumed that it had the

263   same composition as Lake Svartkulp water samples. This assumption is supported by the fact that

264   waters from both lakes have circumneutral pH, low ionic strength (poor buffering capacity) and high

CO_2 overestimation from $HgCl_2$ fixation – Clayer et al.

265   DOC concentration and would therefore behave similarly in presence of acids. Briefly, for each 0.1

266   pH value between pH of 5.4 and 7.3, the carbonate alkalinity was first adjusted by increasing HCO_3

267   concentrations in the input files for PHREEQC to confirm that the water was at equilibrium at the

268   given pH value. Then, the effect of adding 150μL of a half-saturated $HgCl_2$ solution was simulated as

269   described above for Lake Svartkulp. Knowing the new equilibrated pH, after addition of $HgCl_2$, the

270   overestimation of CO_2 concentration in Hg-fixed samples relative to unfixed samples (E, described in

271   Eq. 7 above) can be predicted as described below.

272   Adapting Eq. (1), we obtain:

273
$$[CO_2]_{HgCl_2} = \frac{[H^+]^2_{HgCl_2} C_T}{Z_{HgCl_2}} \qquad \text{(Eq. 8)}$$

274   and

275
$$[CO_2]_i = \frac{[H^+]^2_i C_T}{Z_i} \qquad \text{(Eq. 9)}$$

276   where $[H^+]_i$ is the proton concentration measured in the initial water samples prior to $HgCl_2$ fixation,

277   and $[H^+]_{HgCl_2}$ is the proton concentration estimated by PHREEQC following $HgCl_2$ fixation, and

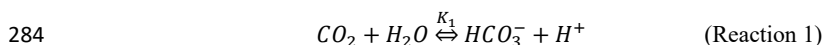278   similarly for Z_i and Z_{HgCl_2} from Eq. (2). Combining Eqs. (6), (8) and (9) we obtain:

279
$$[CO_2]_{ex} = C_T \left(\frac{[H^+]^2_{HgCl_2}}{Z_{HgCl_2}} - \frac{[H^+]^2_i}{Z_i} \right) \qquad \text{(Eq. 10)}$$

280   Hence:

281
$$E = \frac{[CO_2]_{ex}}{[CO_2]_i} = \frac{\left(\frac{[H^+]^2_{HgCl_2}}{Z_{HgCl_2}} - \frac{[H^+]^2_i}{Z_i} \right)}{\frac{[H^+]^2_i}{Z_i}} \qquad \text{(Eq. 11)}$$

282

283   Alternatively, E can also simply be predicted based on the carbonic acid dissociation:

284
$$CO_2 + H_2O \overset{K_1}{\Leftrightarrow} HCO_3^- + H^+ \qquad \text{(Reaction 1)}$$

285   At equilibrium, we have:

286
$$K_1 = \frac{[HCO_3^-][H^+]}{[CO_2]} \qquad \text{(Eq. 12)}$$

287   When pH is decreased upon addition of $HgCl_2$, a fraction (α) of the initial bicarbonate concentration

288    $[HCO_3^-]_i$ is turned into CO_2. This fraction, expressed as $[CO_2]_{ex}$ in Eq. (6) above, can be estimated

289   with Eq. 12 as follows:

CO$_2$ overestimation from HgCl$_2$ fixation – Clayer et al.

290
$$[CO_2]_{ex} = \alpha[HCO_3^-]_i = \frac{\alpha K_1 [CO_2]_i}{[H^+]_i} \qquad \text{(Eq. 13)}$$

291   Introducing the expression of $[CO_2]_{ex}$ from Eq. 13 into Eq. 7 yields:

292
$$\frac{[CO_2]_{ex}}{[CO_2]_i} = E = \frac{\alpha K_1}{[H^+]_i} \qquad \text{(Eq. 14)}$$

293   When the decrease in pH, or acidification, is greater than the buffering capacity of the water: $\alpha = 1$.

294   The value of α cannot exceed 1 because the amount of CO$_2$ produced by a decrease in pH cannot

295   exceed the amount of HCO_3^- initially present. In all the other cases, we have: $\alpha < 1$. For both

296   predictions of E, i.e., with Eqs. 11 and 14, the root-mean-square error (RMSE) and coefficient of

297   determination (R^2) were calculated.

298   Finally, additional sources of CO$_2$ overestimation were investigated by analysing the residuals of the

299   model described by Eq. 11, i.e., the difference between E predicted with Eq. 11 and E determined

300   empirically with Eq. 7. Briefly, residuals were plotted against pH and *in situ* temperature. Residuals

301   were separated in two groups based on the empirical value of $[HCO_3^-]_i - [CO_2]_{ex}$, i.e., the first group

302   had values of $[HCO_3^-]_i - [CO_2]_{ex} \geq a$ while the second group had values of $[HCO_3^-]_i - [CO_2]_{ex} \leq$

303    $-a$ where different values for a were used: 20, 10 or 5 µM. The justification for separating residuals

304   in two groups is that: (i) the first group represents samples for which bicarbonate alkalinity in the

305   original sample is, as expected, higher than CO$_2$ overestimation after HgCl$_2$-fixation, while (ii) the

306   second group represents samples for which bicarbonate alkalinity is not sufficient to explain CO$_2$

307   overestimation after HgCl$_2$-fixation.

308

309   *CO$_2$ diffusion fluxes from Lake Lundebyvannet*

310   The diffusive flux of CO$_2$ (F_{CO_2} in mol m^{-2} d^{-1}) from Lake Lundebyvannet surface water was

311   estimated according to:

312
$$F_{CO_2} = \frac{k_{CO_2}([CO_2] - [CO_2]_{eq})}{1000} \qquad \text{(Eq. 12)}$$

313   where k_{CO_2} is the CO$_2$ transfer velocity in m d^{-1}, $[CO_2]$ is the surface water CO$_2$ concentration (µM),

314   and 1000 is a factor to ensure consistency in the units and $[CO_2]_{eq}$ is the theoretical water CO$_2$

315   concentration (µM) in equilibrium with atmospheric CO$_2$ concentration calculated with Eq. (3) and

316   pCO$_2$ of 416 µatm (see above).

317   The CO$_2$ transfer velocity (k_{CO_2}) was estimated as follows (Vachon & Prairie, 2013):

318
$$k_{CO_2} = k_{600} \left(\frac{600}{Sc_{CO_2}} \right)^{-n} \qquad \text{(Eq. 14)}$$

CO$_2$ overestimation from HgCl$_2$ fixation – Clayer et al.

319　where k_{600} is the gas transfer velocity (m d^{-1}) estimated from empirical wind-based models and Sc_{CO_2}

320　is the CO$_2$ Schmidt number for a given temperature (unitless; Wanninkhof, 2014). We used n values

321　of 0.5 or 2/3 when wind speed was below or above 3.7 m s^{-1}, respectively (Guérin et al., 2007).

322　Empirical k_{600} models included those from Cole & Caraco (1998; $k_{600} = 2.07 + 0.215U_{10}^{1.7}$),

323　Vachon & Prairie (2013; $k_{600} = 2.51 + 1.48U_{10} + 0.39U_{10}\log_{10}LA$) and Crusius & Wanninkhof

324　(2003; power model: $k_{600} = 0.228U_{10}^{2.2} + 0.168$ in cm h^{-1}). U_{10} and LA refer to mean wind speed at

325　10 m in m s^{-1} and lake area in km^2, respectively. Sub-hourly U_{10} data for 2020 was retrieved from a

326　weather station of the Norwegian Meteorological Institute located 1.5 km west of Lake

327　Lundebyvannet (station name: E18 Melleby; ID: SN 3480; 59.546 N, 11.4535E) using the Frost

328　application programming interface (*Frost API*, 2022). Daily, monthly, and yearly (only covering the

329　ice-free season: April-November) F_{CO_2} was estimated using Eq. (12). Daily [CO$_2$] was interpolated

330　from weekly data using a modified Akima spline (makima spline in Matlab® based on Akima, 1974).

331　This interpolation method is known to avoid excessive local undulations.

332　**3. Results and discussion**

333　3.1. Effects of inhibitors and storage time on dissolved gases

334　In the control samples from Lake Svartkulp, the concentration of O$_2$ declined while CO$_2$ increased

335　over time in a close to 1:1 molar ratio, likely reflecting the effect of microbial respiration activity and

336　mineralisation of organic matter (Fig. 1, Table S2). Concentration of O$_2$ in the control decreased from

337　near 300 to below 200 µM (Fig. 1). In the presence of inhibitors, O$_2$ concentrations tended to be

338　slightly higher at t=0 and remained constant or declined only slightly over time to generally remain at

339　or above saturation (280 to 300 µM). Thus, the inhibitors were effective in reducing oxic respiration.

340　The concentration of CO$_2$ in the presence of AgNO$_3$ at t = 0 was not significantly different to the

341　control at t = 0 (Fig 1; paired t-test, *P*>0.1). At t = 0, CO$_2$ concentrations were however much higher

342　in the presence of HgCl$_2$ (135 µM) or CuCl$_2$ (131 µM) than in the control (89 µM; Fig 1, Table S2).

343　This is likely due to an acidification of the poorly buffered (alkalinity 127 µM) and near neutral water

344　(pH=6.73), shifting the carbonate equilibrium from HCO$_3$ to CO$_2$ as also shown by Borges et al.

345　(2019). The increase of CO$_2$ from 130 µM to ~160 µM after 3 weeks in both sample sets preserved

346　with HgCl$_2$ and CuCl$_2$ is not mirrored by a similar decrease in O$_2$. This suggests that oxic respiration

347　is not the main source for this additional 30 µM of CO$_2$ but rather points towards additional

348　acidification of the samples caused by kinetically controlled complexation of Hg^{2+} with dissolved

349　organic matter (Miller et al., 2009). In fact, the relatively slow complexation of Hg^{2+} with organic

350　thiol groups can release two protons (Skyllberg, 2008) and up to three, with some participation of a

351　third weak-acid group (Khwaja et al., 2006). The following decrease in CO$_2$ after 3 months (down to

352　~145 µM) points to other processes. Overall, the addition of HgCl$_2$ or CuCl$_2$ following sampling

353　increased CO$_2$ concentrations by 47% within the first 24h compared to the control and caused further

CO_2 overestimation from $HgCl_2$ fixation – Clayer et al.

354 changes over the three-month storage time, while preservation with $AgNO_3$ yielded CO_2

355 concentrations consistent with the control and caused negligible changes over time (Fig. 1; paired t-

356 test, P>0.1).

357 The concentration of CH_4 ranged between 0.017 and 0.377 μM (Fig. 1), as expected two orders of

358 magnitude smaller than CO_2. At t = 0, the concentration of CH_4 was over 0.2 μM in the presence of

359 inhibitors while it was below saturation in the control (0.03 μM; Fig. 1). CH_4 oversaturation in the

360 preserved samples persisted after three weeks and three months of storage and CH_4 concentration

361 remained constant (Fig. 1, Table S2). Both observations are consistent with the fact that the three

362 preservatives were effective in preserving CH_4 from oxidation. Even at t = 0, i.e., for samples

363 analysed within 24h after sampling, preservatives are required to preserve CH_4 in oxic samples.

CO₂ overestimation from HgCl₂ fixation – Clayer et al.
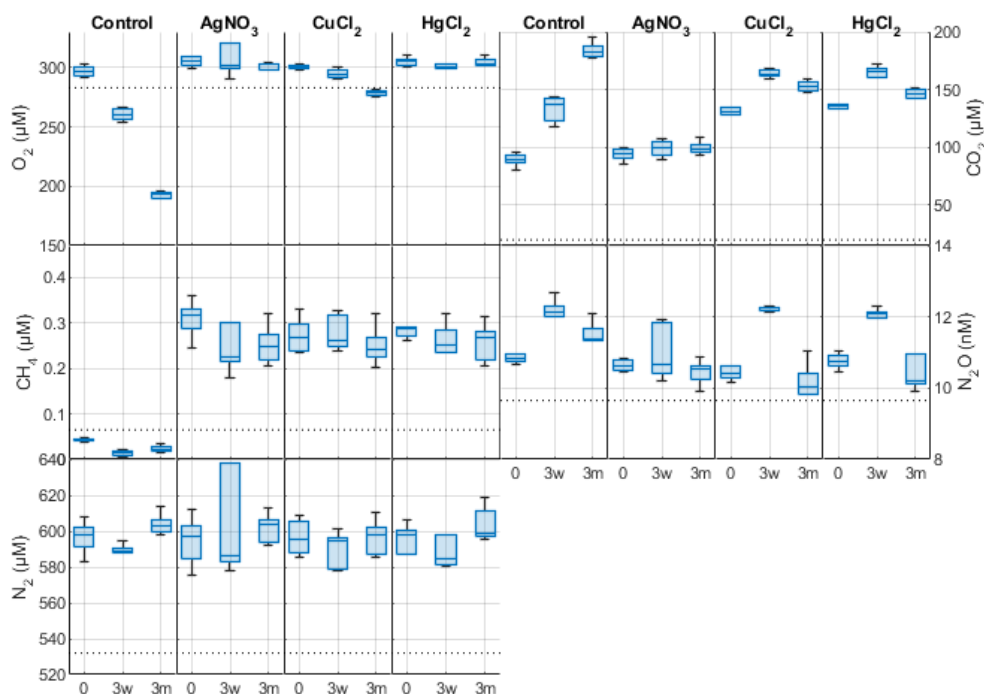
Fig 1. Changes in dissolved O_2, CO_2, CH_4, N_2O and N_2 concentrations (nM or µM) in the absence (control) and presence of different preservatives ($AgNO_3$, $CuCl_2$, $HgCl_2$) at three times (0, day after sample collection; 3w, three weeks after collection; 3m, three months after collection). The horizontal dotted line is the saturated gas concentration corresponding to 100% gas saturation.

CO_2 overestimation from $HgCl_2$ fixation – Clayer et al.

369   In fact, oxic methanotrophy typically show rates in the order of μM day^{-1} (Thottathil et al., 2019; van

370   Grinsven et al., 2021). Hence, a CH_4 consumption of 0.3 μM within 24h in the unpreserved, control

371   water samples is realistic (Fig. 1).

372   The concentration of N_2O ranged between 9.8 and 12.7 nM with only samples preserved with $AgNO_3$

373   showing negligible changes over time (Fig. 1; paired t-test, P>0.1). All the other samples showed

374   consistent patterns with storage time. N_2O concentrations initially increased within the first 3 weeks,

375   followed by a decrease after 3 months. Similar patterns of net N_2O production followed by net

376   consumption were also reported in short-term incubations of seawater from the high latitude Atlantic

377   Ocean, although over much shorter timescales, i.e., 48 and 96h (Rees et al., 2021). The lack of

378   inhibition of N_2O production and consumption in the samples preserved with $HgCl_2$ and $CuCl_2$ can be

379   attributed to the fact that N_2O production tends to increase under increasing acidic conditions

380   (Knowles, 1982; Mørkved et al., 2007; Seitzinger, 1988). In fact, the mole fraction of N_2O produced

381   during denitrification increases compared to N_2 as pH decreases (Knowles, 1982). In summary,

382    $AgNO_3$ appears to be the only preservative inhibiting N_2O cycling, although further tests with a larger

383   range of N_2O concentrations are required to confirm its efficiency.

384   The changes in N_2 were likely within handling and analytical errors and not different in the presence

385   or absence of inhibitors (Fig. 1; Table S2).

386   3.2. Contrasting impacts of $HgCl_2$, $CuCl_2$ and $AgNO_3$ on dissolved CO_2 estimation revealed by

387   chemical speciation modelling

388   The PHREEQC simulation of unpreserved samples, based on concentrations of all major elements

389   (Table S1), predicted a pH of 6.72 (Table 2) which is very close to the measured pH of 6.73 (Table

390   S1). This suggests that chemical information provided to PHREEQC is likely sufficient to describe

391   the system, without having to invoke more complex reactions with dissolved organic matter. The

392   addition of $HgCl_2$ and $CuCl_2$ both caused a significant decrease in pH to 6.40 and 6.45, respectively

393   (Table 2). The proximity of these pH values to the first carbonic acid dissociation constant ($pK_1 =$

394   6.41 at 25°C; Stumm & Morgan, 1996) implies a significant shift in the carbonate equilibrium from

395   HCO_3 to CO_2. In fact, introducing pH and CO_2 concentration values of 6.41–6.45 and 130 μM,

396   respectively, for the samples preserved with $HgCl_2$ and $CuCl_2$ into Eqs. 1 and 2 yields DIC

397   concentrations (C_T) of about 270 μM at t=0. These DIC concentrations are almost equal to those

398   calculated for the control and samples preserved with $AgNO_3$ at t = 0, i.e., with a pH of 6.73 and CO_2

399   concentration of 88 μM. Interestingly, the concentration of CO_2 in the samples preserved with $HgCl_2$

400   and $CuCl_2$ continue to increase up to ~160 μM after 3 weeks. Given that oxic respiration is inhibited

401   (Fig. 1), this additional CO_2 is believed to originate from progressive release of protons following

402   relatively slow complexation of Hg^{2+} with dissolved organic matter (Khwaja et al., 2006; Miller et al.,

CO$_2$ overestimation from HgCl$_2$ fixation – Clayer et al.

403 2009; Skyllberg, 2008). Note that PHREEQC could not predict complexation of Hg^{2+} with dissolved

404 organic matter given that we neglected the effect of dissolved organic matter.

405 In absence of preservatives, none of the common carbonate minerals, including calcite, were

406 associated with a saturation index higher than 1, i.e., dissolution was thermodynamically favourable

407 for all these minerals and no DIC loss was expected (Table 2). However, upon addition of HgCl$_2$ or

408 CuCl$_2$, some carbonate minerals, e.g., HgCO$_3$ or malachite and azurite, respectively, were expected to

409 spontaneously precipitate given their relatively high saturation index values. This observation can

410 explain the consistent decrease in CO$_2$ concentrations observed between three weeks and three months

411 for sampled treated with HgCl$_2$ and CuCl$_2$. Calcite precipitation is typically observed in

412 supersaturated solutions within 48h (Kim et al., 2020). Hence, it is realistic to consider that Hg and Cu

413 carbonate precipitation influenced the CO$_2$ concentration within the preserved samples over the three

414 months of storage time. Impacts of Hg or Cu carbonate precipitation is not evident after three weeks

415 likely because of slow but persistent CO$_2$ production in presence of HgCl$_2$ and CuCl$_2$ related to

416 acidification as described above (Fig. 1). However, after three weeks, this production likely weakens

417 and is counterbalanced by increasing carbonate precipitation.

418 **Table 2.** pH and saturation indexes of selected carbonate minerals estimated by PHREEQC for the

419 unpreserved and preserved samples

| Preservatives	pH	Saturation indexes			
		HgCO$_3$	Cu$_2$(OH)$_2$CO$_3$ - Malachite	Cu$_2$(OH)$_2$CO$_3$ - Azurite	Ag$_2$CO$_3$
Unpreserved	6.72	-2.31	-4.96	-8.71	-16.42
HgCl$_2$	6.40	3.64	-5.89	-10.10	-17.20
CuCl$_2$	6.45	-2.55	2.26	2.11	-17.44
AgNO$_3$	6.71	-2.31	-4.97	-8.73	-4.33

420

421 3.3. Effects of HgCl$_2$ on dissolved CO$_2$ concentration under a range of pH

422 CO$_2$ concentrations in unfixed water samples from Lake Lundebyvannet were significantly lower than

423 in the HgCl$_2$-fixed samples (mean difference: 52 μM; paired t-test; P<0.0001; Table 3). Fixation with

424 HgCl$_2$ caused a general overestimation of CO$_2$ concentration and the saturation deficit (Fig. 2), thus

425 missing out events of CO$_2$ influx (carbon sink) under high photosynthesis activity (high pH; Fig. 2).

426 As for the samples from Lake Svartkulp described above, the overestimation in CO$_2$ concentration

427 likely stems from the acidification by HgCl$_2$ (161 μM added) shifting the carbonate equilibrium

428 towards CO$_2$. In fact, PHREEQC predicted a decrease of 0.6 to 1.8 units of pH related to HgCl$_2$

429 addition (Fig. S1).

430

CO$_2$ overestimation from HgCl$_2$ fixation – Clayer et al.

431
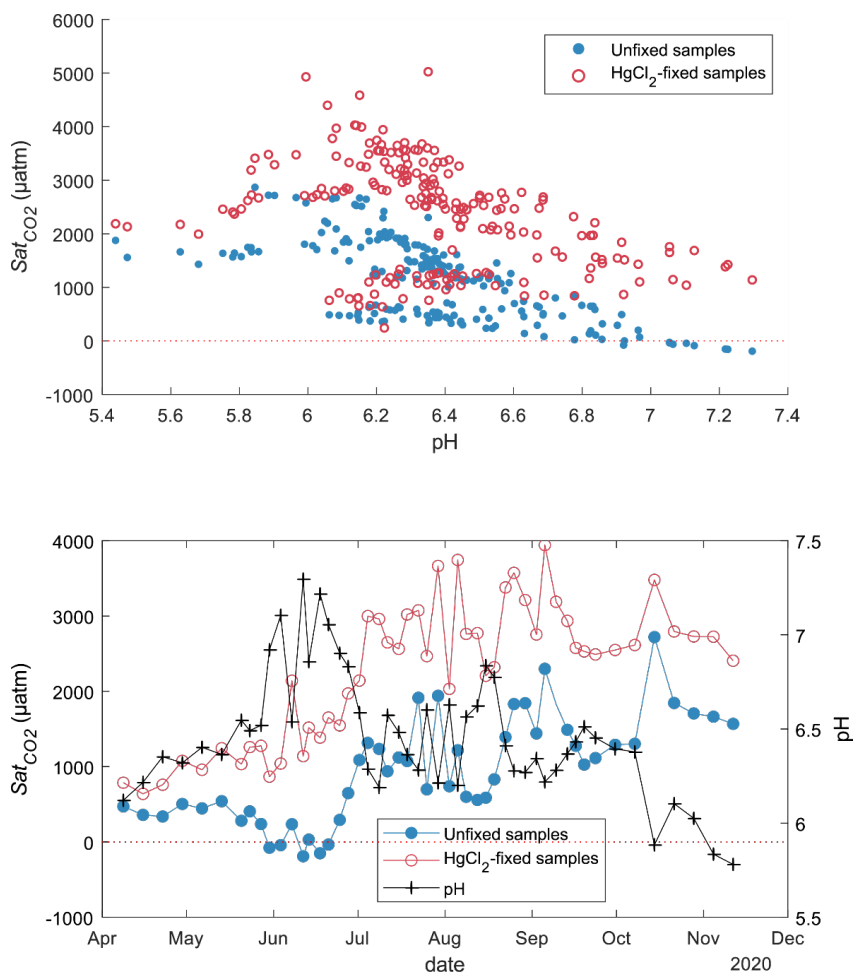
Figure 2. CO$_2$ saturation deficit in Lake Lundebyvannet as a function of pH for all unfixed and

HgCl$_2$-fixed samples (top panel). Timeseries of pH and CO$_2$ saturation deficit of Lake Lundebyvannet

surface water (1-m deep) for unfixed and HgCl$_2$-fixed samples (bottom panel).

CO$_2$ overestimation from HgCl$_2$ fixation – Clayer et al.

435   **Table 3.** CO$_2$ concentrations ([CO$_2$], μM) and diffusion fluxes (F$_{CO2}$, mol m^{-2} d^{-1}) from Lake Lake

436   Lundebyvannet estimated from HgCl$_2$-fixed and unfixed samples following Cole and Caraco (1998)

Preservatives		Apr.	May	Jun.	Jul.	Aug.	Sep.	Oct.	Nov.	Ice-free season
[CO$_2$]	HgCl$_2$	45.3	39.0	18.7	67.9	59.2	85.1	123.4	119.8	66.8
	None	67.9	75.1	74.0	132.9	129.9	149.1	179.3	178.1	121.5
	Diff (%)	50 %	93 %	296 %	96 %	119 %	75 %	45 %	49 %	82 %
F$_{CO2}$	HgCl$_2$	0.10	0.07	0.01	0.15	0.11	0.23	0.37	0.48	0.17
	None	0.20	0.21	0.16	0.34	0.29	0.47	0.57	0.77	0.35
	Diff (%)	97 %	188 %	2163 %	130 %	162 %	99 %	55 %	62 %	108 %

437

438   The pH value of water samples from Lake Lundebyvannet varied between 5.4 and 7.3 (Fig 2 and 3),

439   mainly due to marked variations in phytoplankton photosynthetic activity (Rohrlack et al., 2020). The

440   relative overestimation of CO$_2$ (E) follows an exponential increase with pH and is well reproduced by

441   a simple exponential function ($2.56 \times 10^{-5} \times 10^{1.015 \times pH}$, RMSE=44%, R^2=0.81, p<0.0001; Fig. 3).

442   This exponential increase likely reflects the corresponding decrease in absolute CO$_2$ concentration

443   with pH (Stumm & Morgan, 1981) concomitant here to phytoplankton photosynthesis (Fig. 2). In fact,

444   the exponential increase in CO$_2$ overestimation is easily predicted by Eq. (8) with an equivalent level

445   of accuracy than the optimized exponential function (Fig. 3). Consistently, the relative overestimation

446   of CO$_2$ (E) shows an inverse decrease with $[H^+]$ that is well reproduced by a simple inverse function

447   ($3.25 \times 10^{-5}/[H^+]$; RMSE=44%, R^2=0.81, p<0.0001; Fig. 3) and predicted by Eq. (14), with an α

448   value of 1. Combining Eqs. 7 and 14 and solving it with pH values estimated from PHREEQC (Fig.

449   S1) for α yields values ranging between 0.72 and 0.89 with an average of 0.85. Unexpectedly, this

450   average α value is almost equal to the ratio of the inverse function coefficient and K$_1$, i.e., $\frac{3.25 \times 10^{-5}}{K_1} =$

451   0.87. Hence, the relative overestimation of CO$_2$ (E) caused by HgCl$_2$ fixation is easily predicted by

452   the change in bicarbonate equilibrium knowing the proton release from HgCl$_2$ addition.

453   In waters with higher ionic strength, the release of proton from HgCl$_2$ addition will likely be smaller.

454   PHREEQC can be used to predict it, if sufficient knowledge is gathered on the ionic water

455   composition. Proton release during HgCl$_2$ fixation can be represented by the following reaction:

456    $$HgCl_2 + 2H_2O = Hg(OH)_2 + 2H^+ + 2Cl^- \qquad \text{(Reaction 2)}$$
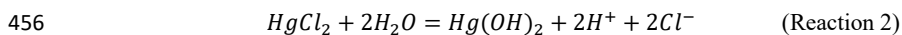
457   From reaction 2, it becomes evident that the initial concentration of chloride in the water samples will

458   likely limit HgCl$_2$ dissociation and proton release. This is a likely mechanism occurring in seawater

459   where HgCl$_2$ has been shown to cause a decrease in pH, although at a negligible level (Chou et al.,

460   2016).

CO$_2$ overestimation from HgCl$_2$ fixation – Clayer et al.

461
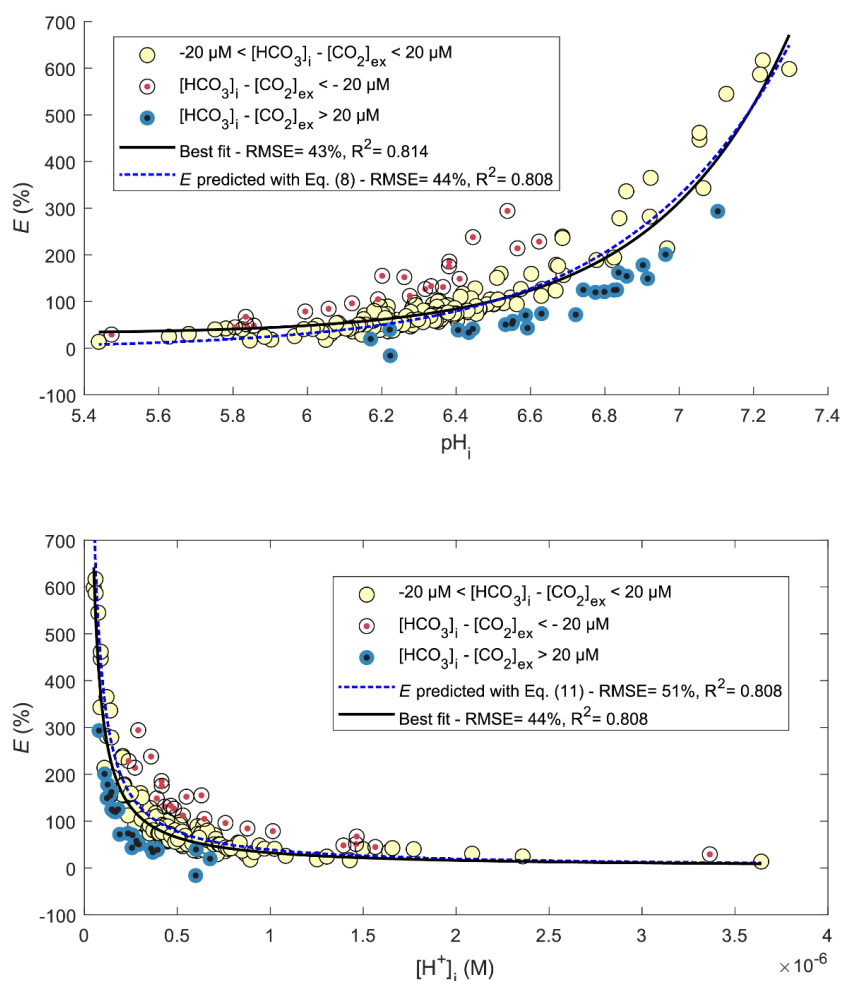
Figure 3. Comparison of observed (circles) and predicted (blue line) relative overestimation (E) of CO$_2$ concentrations caused by HgCl$_2$ fixation in Lake Lundebyvannet samples as a function of pH (top panel) or proton concentration (bottom panel). The black line shows the best fit of the regression analysis. White symbols represent samples for which the bicarbonate concentration in the unfixed samples ($[HCO_3^-]_i$) is nearly equal to CO$_2$ overestimation ($[CO_2]_{ex}$), i.e., ± 20μM, while red and blue symbols represent samples for which initial bicarbonate concentration was lower and higher than the CO$_2$ overestimation, respectively.

CO$_2$ overestimation from HgCl$_2$ fixation – Clayer et al.

469   Figure 2 shows that a range of water samples were associated with a relative CO$_2$ overestimation (E)

470   that substantially deviated from the overestimation predicted with Eq. 11 (red and blue symbols in

471   Fig. 3). In fact, some samples had a higher initial bicarbonate content ($[HCO_3^-]_i$) than the excess CO$_2$

472   concentration ($[CO_2]_{ex}$), while other showed the opposite. The former case (blue symbols in Fig. 3)

473   can easily be explained by a higher buffering capacity of the sampled water, i.e., a higher pH after

474   HgCl$_2$-fixation than that predicted by PHREEQC related to a different water composition. Indeed, the

475   concentration of major elements in the water from Lake Lundebyvannet may vary significantly over

476   time, and in absence of data, we considered that the water composition, except for DIC, pH and

477   HgCl$_2$, was constant over time. By contrast, samples associated with $[CO_2]_{ex}$ being larger than

478   $[HCO_3^-]_i$ are more enigmatic. In order to shed light on possible explanations, we visually inspected

479   trends between empirical deviations from predictions, i.e., residuals, and *in situ* temperature or pH.

480   Absolute values of residuals showed a progressive increase with pH and *in situ* temperature which is

481   in agreement with decreasing precision of the headspace method with increasing temperature and pH

482   (Koschorreck et al., 2021). In fact, CO$_2$ is less soluble at higher temperature, hence more gas can

483   evade during sampling, and thus the error increases with *in situ* temperature. In addition, at higher pH,

484   CO$_2$ concentration decreases and consequently the absolute error on CO$_2$ quantification becomes

485   larger relative to measured CO$_2$ concentration. Interestingly, many of the high residual values were

486   not evenly distributed across the year, nor across the summer and were rather associated with only a

487   few specific sampling events during summer (Fig. S2). This suggests that gas loss could have

488   occurred due to high ambient temperature in the field. Water associated with $[CO_2]_{ex}$ being larger

489   than $[HCO_3^-]_i$ (red symbols in Fig. 3 and S4) could have been subject to a larger gas loss in the

490   samples collected for DIC analysis than the samples for GC analysis. On the other hand, loss of gas

491   was likely larger for samples for GC analysis than for DIC analysis for water associated with

492   $[HCO_3^-]_i$ being larger than $[CO_2]_{ex}$ (blue symbols in Fig. 3 and Fig. S2). In addition to gas losses and

493   temperature effects, errors in pH measurements can also cause a large misestimation of CO$_2$

494   concentration from DIC analysis, and this error increases exponentially with pH following the shift in

495   carbonate equilibrium. In summary, our analysis is consistent with that of Koschorreck et al. (2021)

496   showing that errors in the determination of CO$_2$ concentrations are smaller at lower pH and lower

497   temperature (Fig. S2).

498   3.4. Implications for the estimation of lake and reservoir C cycling

499   Using HgCl$_2$ (or CuCl$_2$) to preserve dissolved gas samples in poorly buffered water samples would

500   have large impacts on CO$_2$ concentrations with considerable risk of leading to incorrect

501   interpretations. In fact, over the ice-free season, average CO$_2$ concentrations in Lake Lundebyvannet

502   determined following HgCl$_2$-fixation and GC analysis were 82% higher than those obtained from DIC

503   analyses (Table 3; Fig. 4 and S3). CO$_2$ concentrations obtained from HgCl$_2$-fixed samples created the

504   illusion that Lake Lundebyvannet was a steady net source of CO$_2$ to the atmosphere over the ice-free

CO_2 overestimation from $HgCl_2$ fixation – Clayer et al.

505   season with large CO_2 saturation deficit (Fig. 3) while, in reality, the lake switched from being a net

506   source in May, to a net sink over a few weeks in June, and returning to a net source in July (Fig. 4 and

507   S3). Indeed, monthly CO_2 overestimation related to $HgCl_2$-fixation reached about 300% in June

508   (Table 3). Propagating this overestimation into the estimates of CO_2 diffusion fluxes with typical

509   wind-based models yields overestimation of CO_2 fluxes of 108–112% over the ice-free season and up

510   to 2100% in June (Tables 3 and S3). Hence, interpreting CO_2 data without correcting for CO_2

511   overestimation caused by $HgCl_2$-fixation leads to negligence of the role of photosynthesis in lake C

512   cycling with major implications for current and future predictions of lake CO_2 emissions.

513   **Conclusion**

514   Mercury is a potent neurotoxin for humans and toxic for the environment and its use should be

515   discouraged, notably following the Minamata convention on mercury, a global treaty ratified by 126

516   countries (16 December 2020) to protect human health and the environment from the adverse effects

517   of mercury. This study further questions the use of $HgCl_2$ for preservation of poorly buffered (low

518   ionic strength) water samples with high DOC concentration for analysis of dissolved gases in the

519   laboratory. Although $CuCl_2$ is less toxic, it behaved similarly to $HgCl_2$ and cannot be recommend. In

520   fact, both chlorinated inhibitors caused a significant decrease in pH shifting the carbonate equilibrium

521   towards CO_2 and are also suspected to promote carbonate precipitation over long-term storage. The

522   only promising inhibitor tested in this study was $AgNO_3$ notably for dissolved CO_2, CH_4 and N_2O.

523   Silver nitrate may be a suitable substitute for $HgCl_2$, but further tests should be carried out with a

524   range of inhibitor concentration and more diverse water samples. The use of chemical inhibitors may

525   not be the best approach. Alternatives exist, such as directly measuring gas concentrations *in situ* with

526   sensors, or sampling the headspace out in the field, and bringing back gas samples (e.g., Cole et al.,

527   1994; Karlsson et al., 2013; Kling et al., 1991; Valiente et al., 2022), rather than water samples, to the

528   lab for gas chromatography analyses. However, care must be taken to know the exact equilibration

529   temperature (Koschorreck et al., 2021).

530
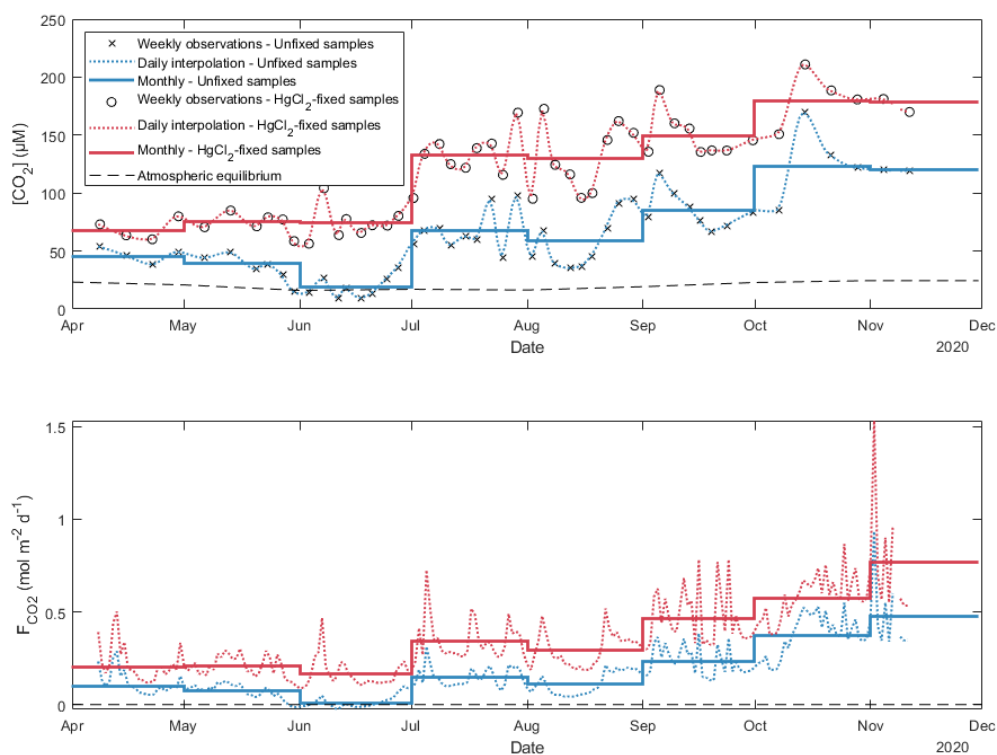
Figure 4. Daily and monthly surface CO_2 concentrations ($[CO_2]$; top panel) and diffusion fluxes
(F_{CO2}; bottom panel) at the water-atmosphere interface from Lake Lundebyvannet. Daily $[CO_2]$ was
interpolated from weekly data using a modified spline (see text for details). Diffusion fluxes were
calculated following Cole & Caraco (1998).

CO_2 overestimation from $HgCl_2$ fixation – Clayer et al.

535 We further advise against interpretation of CO_2 concentration data from low ionic strength, circum-

536 neutral water samples preserved with $HgCl_2$ or $CuCl_2$. The overestimation of CO_2 concentration

537 caused by $HgCl_2$ can mask the effect of photosynthesis on lake carbon balance, creating the illusion

538 that lakes are net CO_2 sources when they are net CO_2 sinks. Our analysis from Lake Lundebyvannet

539 shows that $HgCl_2$ fixation led to an overestimation of the CO_2 concentration by a factor of 1.8, on

540 average, but approaching a factor of 4 during the peak photosynthetic period. An even larger impact is

541 expected on CO_2 diffusive fluxes which were overestimated by a factor of 2 on average and up to a

542 factor of >20 during peak photosynthesis. Interpreting such data would have underestimated the

543 current and future role of aquatic photosynthesis.

544 **Data availability**

545 All data supporting this study will be made available on a permanent repository upon acceptance, e.g.,

546 Hydroshare.

547 **Author contribution**

548 JET, AK, and TR supervised and PD, KN and FC contributed to the study design. JET, KN and TR

549 carried out the experiments. PD and TR performed the chemical analyses. JET and FC wrote the first

550 draft. FC performed the modelling, data, and statistical analyses, and drafted the figures. All co-

551 authors edited the manuscript.

552 **Competing interests**

553 The contact author has declared that none of the authors has any competing interests.

554 **Acknowledgements**

558

559 **References**

560 Akima, H. (1974). A method of bivariate interpolation and smooth surface fitting based on local
561 procedures. *Communications of the ACM*, *17*(1), 18–20.
562 https://doi.org/10.1145/360767.360779
563 Allison, J., Brown, D., & Novo-Gradac, K. (1991). *MINTEQA2/PRODEFA2, a geochemical
564 assessment model for environmental systems: Version 3. 0 user's manual*. GA: US
565 Environmental Protection Agency.
566 Borges, A. V., Darchambeau, F., Lambert, T., Morana, C., Allen, G. H., Tambwe, E., Toengaho
567 Sembaito, A., Mambo, T., Nlandu Wabakhangazi, J., Descy, J.-P., Teodoru, C. R., &
568 Bouillon, S. (2019). Variations in dissolved greenhouse gases (CO_2, CH_4, N_2O) in the Congo

569   River network overwhelmingly driven by fluvial-wetland connectivity. *Biogeosciences*,
570   *16*(19), 3801–3834. https://doi.org/10.5194/bg-16-3801-2019
571   Carroll J.J., Slupsky J.D. & Mather A.E. (1991) The solubility of carbon dioxide in water at low
572   pressure. *Journal of Physical and Chemical Reference Data,* **20,** 1201-1209.
573   https://doi.org/10.1063/1.555900
574   Chen, C. Y., Driscoll, C., Eagles-Smith, C. A., Eckley, C. S., Gay, D. A., Hsu-Kim, H., Keane, S. E.,
575   Kirk, J. L., Mason, R. P., Obrist, D., Selin, H., Selin, N. E., & Thompson, M. R. (2018). A
576   Critical Time for Mercury Science to Inform Global Policy. *Environmental Science &*
577   *Technology*, *52*(17), 9556–9561. https://doi.org/10.1021/acs.est.8b02286
578   Chen H., Johnston R.C., Mann B.F., Chu R.K., Tolic N., Parks J.M. & Gu B. (2017) Identification of
579   mercury and dissolved organic matter complexes using ultrahigh resolution mass
580   spectrometry. *Environmental Science & Technology Letters,* **4,** 59-65.
581   https://doi.org/10.1021/acs.estlett.6b00460
582   Chou W.C., Gong G.C., Yang C.Y. & Chuang K.Y. (2016) A comparison between field and
583   laboratory pH measurements for seawater on the East China Sea shelf. *Limnology and*
584   *Oceanography-Methods,* **14,** 315-322. https://doi.org/10.1002/lom3.10091
585   Ciavatta L. & Grimaldi M. (1968) The hydrolysis of mercury(II) chloride, HgCl2. *Journal of*
586   *Inorganic and Nuclear Chemistry,* **30,** 563-581. https://doi.org/10.1016/0022-1902(68)80483-
587   X
588   Clayer, F., Thrane, J.-E., Brandt, U., Dörsch, P., & de Wit, H. A. (2021). Boreal Headwater
589   Catchment as Hot Spot of Carbon Processing From Headwater to Fjord. *Journal of*
590   *Geophysical Research: Biogeosciences*, *126*(12), e2021JG006359.
591   https://doi.org/10.1029/2021JG006359
592   Cole, J. J., Caraco, N. F., Kling, G. W., & Kratz, T. K. (1994). Carbon Dioxide Supersaturation in the
593   Surface Waters of Lakes. *Science*, *265*(5178), Article 5178.
594   https://doi.org/10.1126/science.265.5178.1568
595   Cole, J. J., & Caraco, N. F. (1998). Atmospheric exchange of carbon dioxide in a low-wind
596   oligotrophic lake measured by the addition of SF6. *Limnology and Oceanography*, *43*(4),
597   Article 4. https://doi.org/10.4319/lo.1998.43.4.0647
598   Crusius, J., & Wanninkhof, R. (2003). Gas transfer velocities measured at low wind speed over a lake.
599   *Limnology and Oceanography*, *48*(3), Article 3. https://doi.org/10.4319/lo.2003.48.3.1010
600   Deheyn, D. D., Bencheikh-Latmani, R., & Latz, M. I. (2004). Chemical speciation and toxicity of
601   metals assessed by three bioluminescence-based assays using marine organisms.
602   *Environmental Toxicology*, *19*(3), 161–178. https://doi.org/10.1002/tox.20009
603   de Wit, H. A., Garmo, Ø. A., Jackson-Blake, L. A., Clayer, F., Vogt, R. D., Austnes, K., Kaste, Ø.,
604   Gundersen, C. B., Guerrero, J. L., & Hindar, A. (2023). Changing Water Chemistry in One
605   Thousand Norwegian Lakes During Three Decades of Cleaner Air and Climate Change.
606   Global Biogeochemical Cycles, 37(2), e2022GB007509.
607   https://doi.org/10.1029/2022GB007509
608   Dickson A.G., Sabine C.L. & Christian J.R. (2007) *Guide to best practices for ocean CO2*
609   *measurements,* North Pacific Marine Science Organization.
610   Duan, Z., & Mao, S. (2006). A thermodynamic model for calculating methane solubility, density and
611   gas phase composition of methane-bearing aqueous fluids from 273 to 523K and from 1 to
612   2000bar. *Geochimica et Cosmochimica Acta*, *70*(13), Article 13.
613   https://doi.org/10.1016/j.gca.2006.03.018
614   Foti C., Giuffre O., Lando G. & Sammartano S. (2009) Interaction of inorganic mercury (II) with
615   polyamines, polycarboxylates, and amino acids. *Journal of Chemical & Engineering Data,*
616   **54,** 893-903. https://doi.org/10.1021/je800685c
617   *Frost API*. (2022). https://frost.met.no/index.html
618   Guérin, F., Abril, G., Richard, S., Burban, B., Reynouard, C., Seyler, P., & Delmas, R. (2006).
619   Methane and carbon dioxide emissions from tropical reservoirs: Significance of downstream
620   rivers. *Geophysical Research Letters*, *33*(21). https://doi.org/10.1029/2006GL027929
621   Guérin, F., Abril, G., Serça, D., Delon, C., Richard, S., Delmas, R., Tremblay, A., & Varfalvy, L.
622   (2007). Gas transfer velocities of CO2 and CH4 in a tropical reservoir and its river

623   downstream. *Journal of Marine Systems*, *66*(1), Article 1.
624   https://doi.org/10.1016/j.jmarsys.2006.03.019
625   Halmi, M. I. E., Kassim, A., & Shukor, M. Y. (2019). Assessment of heavy metal toxicity using a
626   luminescent bacterial test based on Photobacterium sp. Strain MIE. *Rendiconti Lincei. Scienze*
627   *Fisiche e Naturali*, *30*(3), 589–601. https://doi.org/10.1007/s12210-019-00809-5
628   Hamme R.C. & Emerson S.R. (2004) The solubility of neon, nitrogen and argon in distilled water and
629   seawater. *Deep-Sea Research Part I-Oceanographic Research Papers*, **51,** 1517-1528.
630   https://doi.org/10.1016/j.dsr.2004.06.009
631   Hassen A., Saidi N., Cherif M. & Boudabous A. (1998) Resistance of environmental bacteria to heavy
632   metals. *Bioresource technology*, **64,** 7-15. https://doi.org/10.1016/S0960-8524(97)00161-2
633   Hessen, D. O., Håll, J. P., Thrane, J.-E., & Andersen, T. (2017). Coupling dissolved organic carbon,
634   CO2 and productivity in boreal lakes. *Freshwater Biology*, *62*(5), 945–953.
635   https://doi.org/10.1111/fwb.12914
636   Hilgert, S., Scapulatempo Fernandes, C. V., & Fuchs, S. (2019). Redistribution of methane emission
637   hot spots under drawdown conditions. *Science of The Total Environment*, *646*, 958–971.
638   https://doi.org/10.1016/j.scitotenv.2018.07.338
639   Horvatić J. & Peršić V. (2007) The effect of Ni 2+, Co 2+, Zn 2+, Cd 2+ and Hg 2+ on the growth
640   rate of marine diatom Phaeodactylum tricornutum Bohlin: microplate growth inhibition test.
641   *Bulletin of Environmental Contamination and Toxicology*, **79,** 494-498.
642   https://doi.org/10.1007/s00128-007-9291-7
643   IEA. (2020). *Key World Energy Statistics 2020*. IEA, International Energy Agency.
644   https://www.iea.org/reports/key-world-energy-statistics-2020
645   Karlsson, J., Giesler, R., Persson, J., & Lundin, E. (2013). High emission of carbon dioxide and
646   methane during ice thaw in high latitude lakes. *Geophysical Research Letters*, *40*(6), Article
647   6. https://doi.org/10.1002/grl.50152
648   Khwaja, A. R., Bloom, P. R., & Brezonik, P. L. (2006). Binding Constants of Divalent Mercury
649   (Hg2+) in Soil Humic Acids and Soil Organic Matter. *Environmental Science & Technology*,
650   *40*(3), 844–849. https://doi.org/10.1021/es051085c
651   Kim, D., Mahabadi, N., Jang, J., & van Paassen, L. A. (2020). Assessing the Kinetics and Pore-Scale
652   Characteristics of Biological Calcium Carbonate Precipitation in Porous Media using a
653   Microfluidic Chip Experiment. *Water Resources Research*, *56*(2), e2019WR025420.
654   https://doi.org/10.1029/2019WR025420
655   Kling, G. W., Kipphut, G. W., & Miller, M. C. (1991). Arctic Lakes and Streams as Gas Conduits to
656   the Atmosphere: Implications for Tundra Carbon Budgets. *Science*, *251*(4991), 298–301.
657   https://doi.org/10.1126/science.251.4991.298
658   Knowles, R. (1982). Denitrification. *Microbiological Reviews*, *46*(1), 43–70.
659   https://doi.org/10.1128/mr.46.1.43-70.1982
660   Koschorreck, M., Prairie, Y. T., Kim, J., & Marcé, R. (2021). Technical note: CO₂ is not like CH₄ –
661   limits of and corrections to the headspace method to analyse *p*CO₂ in fresh water.
662   *Biogeosciences*, *18*(5), 1619–1627. https://doi.org/10.5194/bg-18-1619-2021
663   Larrañaga, M., Lewis, R., & Lewis, R. (2016). Hawley's Condensed Chemical Dictionary, Sixteenth
664   Edition. i–xiii. https://doi.org/10.1002/9781119312468.fmatter
665   Liang X., Lu X., Zhao J., Liang L., Zeng E.Y. & Gu B. (2019) Stepwise reduction approach reveals
666   mercury competitive binding and exchange reactions within natural organic matter and mixed
667   organic ligands. *Environmental Science & Technology*, **53,** 10685-10694.
668   https://doi.org/10.1021/acs.est.9b02586
669   Machado Damazio, J., Cordeiro Geber de Melo, A., Piñeiro Maceira, M. E., Medeiros, A., Negrini,
670   M., Alm, J., Schei, T. A., Tateda, Y., Smith, B., & Nielsen, N. (2012). *Guidelines for*
671   *quantitative analysis of net GHG emissions from reservoirs: Volume 1: Measurement*
672   *Programmes and Data Analysis*. International Energy Agency (IEA).
673   https://www.ieahydro.org/media/992f6848/GHG_Guidelines_22October2012_Final.pdf
674   Magen, C., Lapham, L. L., Pohlman, J. W., Marshall, K., Bosman, S., Casso, M., & Chanton, J. P.
675   (2014). A simple headspace equilibration method for measuring dissolved methane.
676   Limnology and Oceanography: Methods, 12(9), 637–650.
677   https://doi.org/10.4319/lom.2014.12.637

678   Miller, C. L., Southworth, G., Brooks, S., Liang, L., & Gu, B. (2009). Kinetic Controls on the
679   Complexation between Mercury and Dissolved Organic Matter in a Contaminated
680   Environment. *Environmental Science & Technology*, *43*(22), 8548–8553.
681   https://doi.org/10.1021/es901891t
682   Millero F.J., Huang F. & Laferiere A.L. (2002) Solubility of oxygen in the major sea salts as a
683   function of concentration and temperature. *Marine Chemistry,* **78,** 217-230.
684   https://doi.org/10.1016/S0304-4203(02)00034-8
685   Mørkved, P. T., Dörsch, P., & Bakken, L. R. (2007). The N2O product ratio of nitrification and its
686   dependence on long-term changes in soil pH. *Soil Biology and Biochemistry*, *39*(8), 2048–
687   2057. https://doi.org/10.1016/j.soilbio.2007.03.006
688   NILU. (2022). *EBAS*. https://ebas-data.nilu.no/Default.aspx
689   Nowack, B., Krug, H. F., & Height, M. (2011). 120 Years of Nanosilver History: Implications for
690   Policy Makers. Environmental Science & Technology, 45(4), 1177–1183.
691   https://doi.org/10.1021/es103316q
692   NPIRS. (2023). *Purdue University.* https://www.npirs.org/public
693   Okuku, E. O., Bouillon, S., Tole, M., & Borges, A. V. (2019). Diffusive emissions of methane and
694   nitrous oxide from a cascade of tropical hydropower reservoirs in Kenya. *Lakes &*
695   *Reservoirs: Science, Policy and Management for Sustainable Use*, *24*(2), 127–135.
696   https://doi.org/10.1111/lre.12264
697   Parkhurst, D. L., & Appelo, C. A. J. (2013). *Description of input and examples for PHREEQC version*
698   *3—A computer program for speciation, batch-reaction, one-dimensional transport, and*
699   *inverse geochemical calculations: U.S. Geological Survey Techniques and Methods* (book 6,
700   chap. A43; p. 497). USGS. http://pubs.usgs.gov/tm/06/a43/
701   Powell K.J., Brown P.L., Byrne R.H., Gajda T., Hefter G., Sjöberg S. & Wanner H. (2004) Chemical
702   speciation of Hg (II) with environmental inorganic ligands. *Australian Journal of Chemistry,*
703   **57,** 993-1000. https://doi.org/10.1071/CH04063
704   Rai L.C., Gaur J.P. & Kumar H.D. (1981) Phycology and heavy-metal pollution. *Biological Reviews,*
705   **56,** 99-151. https://doi.org/10.1111/j.1469-185X.1981.tb00345.x
706   Rees, A. P., Brown, I. J., Jayakumar, A., Lessin, G., Somerfield, P. J., & Ward, B. B. (2021).
707   Biological nitrous oxide consumption in oxygenated waters of the high latitude Atlantic
708   Ocean. *Communications Earth & Environment*, *2*(1), Article 1.
709   https://doi.org/10.1038/s43247-021-00104-y
710   Rohrlack T., Frostad P., Riise G. & Hagman C.H.C. (2020) Motile phytoplankton species such as
711   Gonyostomum semen can significantly reduce CO_2 emissions from boreal lakes.
712   *Limnologica,* **84,** 125810. https://doi.org/10.1016/j.limno.2020.125810
713   Schubert, C. J., Diem, T., & Eugster, W. (2012). Methane Emissions from a Small Wind Shielded
714   Lake Determined by Eddy Covariance, Flux Chambers, Anchored Funnels, and Boundary
715   Model Calculations: A Comparison. *Environmental Science & Technology*, *46*(8), 4515–
716   4522. https://doi.org/10.1021/es203465x
717   Seitzinger, S. P. (1988). Denitrification in freshwater and coastal marine ecosystems: Ecological and
718   geochemical significance. *Limnology and Oceanography*, *33*(4part2), 702–724.
719   https://doi.org/10.4319/lo.1988.33.4part2.0702
720   Silver S. & Phung L.T. (2005) A bacterial view of the periodic table: genes and proteins for toxic
721   inorganic ions. *Journal of Industrial Microbiology & Biotechnology,* **32,** 587-605.
722   https://doi.org/10.1007/s10295-005-0019-6
723   Skyllberg, U. (2008). Competition among thiols and inorganic sulfides and polysulfides for Hg and
724   MeHg in wetland soils and sediments under suboxic conditions: Illumination of controversies
725   and implications for MeHg net production. *Journal of Geophysical Research:*
726   *Biogeosciences*, *113*(G2). https://doi.org/10.1029/2008JG000745
727   Stumm W. & Morgan J.J. (1981) *Aquatic Chemistry. An introduction emphasizing chemical*
728   *equilibria in natural waters,* Wiley Interscience, New York.
729   Stumm, W., & Morgan, J. J. (1996). *Aquatic chemistry: Chemical equilibria and rates in natural*
730   *waters* (3rd ed.). Wiley.

731 Taipale S.J. & Sonninen E. (2009) The influence of preservation method and time on the delta C-13
732   value of dissolved inorganic carbon in water samples. *Rapid Communications in Mass
733   Spectrometry,* **23,** 2507-2510. https://doi.org/10.1002/rcm.4072
734 Takahashi H.A., Handa H., Sugiyama A., Matsushita M., Kondo M., Kimura H. & Tsujimura M.
735   (2019) Filtration and exposure to benzalkonium chloride or sodium chloride to preserve water
736   samples for dissolved inorganic carbon analysis. *Geochemical Journal,* **53,** 305-318.
737   https://doi.org/10.2343/geochemj.2.0570
738 Thottathil, S. D., Reis, P. C. J., & Prairie, Y. T. (2019). Methane oxidation kinetics in northern
739   freshwater lakes. *Biogeochemistry*, *143*(1), Article 1. https://doi.org/10.1007/s10533-019-
740   00552-x
741 Tipping E. (2007) Modelling the interactions of Hg(II) and methylmercury with humic substances
742   using WHAM/Model VI. *Applied Geochemistry,* **22,** 1624-1635.
743 Tørseth, K., Aas, W., Breivik, K., Fjæraa, A. M., Fiebig, M., Hjellbrekke, A. G., Lund Myhre, C.,
744   Solberg, S., & Yttri, K. E. (2012). Introduction to the European Monitoring and Evaluation
745   Programme (EMEP) and observed atmospheric composition change during
746   1972–2009. *Atmospheric Chemistry and Physics*, *12*(12), 5447–5481.
747   https://doi.org/10.5194/acp-12-5447-2012
748 Ullmann, F., Gerhartz, W., Yamamoto, Y. S., Campbell, F. T., Pfefferkorn, R., & Rounsaville, J. F.
749   (1985). Ullmann's encyclopedia of industrial chemistry (5th, completely rev. ed ed.). VCH.
750 UNESCO/IHA. (2008). *Assessment of the GHG status of freshwater reservoirs: Scoping paper*
751   (IHP/GHG-WG/3; p. 28). UNESCO/IHA, International Hydropower Association -
752   International Hydrological Programme, Working Group on Greenhouse Gas Status of
753   Freshwater Reservoirs. https://unesdoc.unesco.org/ark:/48223/pf0000181713
754 UNESCO/IHA. (2010). *GHG Measurement Guidelines for Freshwater Reservoirs* (p. 154).
755   UNESCO/IHA, International Hydropower Association.
756   https://www.hydropower.org/publications/ghg-measurement-guidelines-for-freshwater-
757   reservoirs
758 Vachon, D., & Prairie, Y. T. (2013). The ecosystem size and shape dependence of gas transfer
759   velocity versus wind speed relationships in lakes. *Canadian Journal of Fisheries and Aquatic
760   Sciences*, *70*(12), Article 12. https://doi.org/10.1139/cjfas-2013-0241
761 Valiente, N., Eiler, A., Allesson, L., Andersen, T., Clayer, F., Crapart, C., Dörsch, P., Fontaine, L.,
762   Heuschele, J., Vogt, R., Wei, J., de Wit, H. A., & Hessen, D. O. (2022). *Catchment properties
763   as predictors of greenhouse gas concentrations across a gradient of boreal lakes*.
764   *10*(880619). https://doi.org/10.3389/fenvs.2022.880619
765 van Grinsven, S., Oswald, K., Wehrli, B., Jegge, C., Zopfi, J., Lehmann, M. F., & Schubert, C. J.
766   (2021). Methane oxidation in the waters of a humic-rich boreal lake stimulated by
767   photosynthesis, nitrite, Fe(III) and humics. *Biogeosciences*, *18*(10), 3087–3101.
768   https://doi.org/10.5194/bg-18-3087-2021
769 Wanninkhof, R. (2014). Relationship between wind speed and gas exchange over the ocean revisited.
770   *Limnology and Oceanography: Methods*, *12*(6), Article 6.
771   https://doi.org/10.4319/lom.2014.12.351
772 Weiss R.F. & Price B.A. (1980) Nitrous oxide solubility in water and seawater. *Marine Chemistry,* **8,**
773   347-359. https://doi.org/10.1016/0304-4203(80)90024-9
774 Wilhelm E., Battino R. & Wilcock R.J. (1977) Low-pressure solubility of gases in liquid water.
775   *Chemical Reviews,* **77,** 219-262. https://doi.org/10.1021/cr60306a003
776 Wilson J., Munizzi J. & Erhardt A.M. (2020) Preservation methods for the isotopic composition of
777   dissolved carbon species in non-ideal conditions. *Rapid Communications in Mass
778   Spectrometry,* **34.** https://doi.org/10.1002/rcm.8903
779 Xiao, S., Yang, H., Liu, D., Zhang, C., Lei, D., Wang, Y., Peng, F., Li, Y., Wang, C., Li, X., Wu, G.,
780   & Liu, L. (2014). Gas transfer velocities of methane and carbon dioxide in a subtropical
781   shallow pond. *Tellus B: Chemical and Physical Meteorology*, *66*(1), 23795.
782   https://doi.org/10.3402/tellusb.v66.23795
783 Xu F.F. & Imlay J.A. (2012) Silver(I), Mercury(II), Cadmium(II), and Zinc(II) Target Exposed
784   Enzymic Iron-Sulfur Clusters when They Toxify Escherichia coli. *Applied and Environmental
785   Microbiology,* **78,** 3614-3621. https://doi.org/10.1128/aem.07368-11

CO_2 overestimation from $HgCl_2$ fixation – Clayer et al.

786   Yamamoto S., Alcauskas J.B. & Crozier T.E. (1976) Solubility of methane in distilled water and
787   seawater. *Journal of Chemical and Engineering Data,* **21,** 78-80.
788   https://doi.org/10.1021/je60068a029
789   Yan, F., Sillanpää, M., Kang, S., Aho, K. S., Qu, B., Wei, D., Li, X., Li, C., & Raymond, P. A.
790   (2018). Lakes on the Tibetan Plateau as Conduits of Greenhouse Gases to the Atmosphere.
791   *Journal of Geophysical Research: Biogeosciences*, *123*(7), 2091–2103.
792   https://doi.org/10.1029/2017JG004379
793   Yang H., Andersen T., Dorsch P., Tominaga K., Thrane J.E. & Hessen D.O. (2015) Greenhouse gas
794   metabolism in Nordic boreal lakes. *Biogeochemistry,* **126,** 211-225.
795   https://doi.org/10.1007/s10533-015-0154-8

796